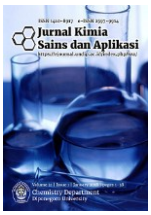
ISSN: 1410-8917
e-ISSN: 2597-9914

Jurnal Kimia Sains dan Aplikasi 29 (9) (2026): 608-617

Jurnal Kimia Sains dan Aplikasi
Journal of Scientific and Applied Chemistry

Journal homepage: http://ejournal.undip.ac.id/index.php/ksa



Biodiesel Synthesis from Palm Acid Oil with Sulfonated Activated Carbon Catalyst from Rice Husk

Haryono [1,2,*], Nova Rachmadona [2], Hersandy Dayu Kusuma [2], Irwan Kurnia [1], Iman Rahayu [1], Atiek Rostika Noviyanti [1]

[1] Department of Chemistry, Faculty of Mathematics and Natural Sciences, Universitas Padjadjaran, Jatinangor, Indonesia
[2] Department of Applied Sciences, School of Vocational Studies, Universitas Padjadjaran, Jatinangor, Indonesia

* Corresponding author: haryono@unpad.ac.id

https://doi.org/10.14710/jksa.29.9.608-617

Article Info

Article history:

Received: 14th June 2026
Revised: 20th September 2026
Accepted: 25th September 2026
Online: 30th October 2026

Keywords:
biodiesel; sulfonated activated carbon; palm acid oil; alkali fusion; rice husk

Abstract

The use of non-edible oil as a raw material and the use of biomass waste as a catalyst in the biodiesel production process is a strategic step due to the various advantages it offers. Palm acid oil (PAO), which is a waste from the palm oil processing industry, has great potential to be used as a raw material in biodiesel production, while rice husks can be processed and their properties modified to be used as a catalyst in the biodiesel formation reaction. This study aims to determine the characteristics and catalytic performance of sulfonated activated carbon from rice husks in the synthesis of biodiesel from PAO. Biodiesel was synthesized at various molar ratios of PAO to methanol of (1:16), (1:24), and (1:32). The reaction was carried out at a temperature of 65°C for 2 hours, with catalyst levels varied at 2, 3, and 5%. The results of the study showed that the best catalytic performance of sulfonated rice husk activated carbon in the synthesis of biodiesel from PAO was achieved at a mole ratio of PAO to methanol of (1:32) and a catalyst content of 2%. Under these synthesis conditions, the highest degree of conversion of free fatty acids into biodiesel was achieved, namely 85.08%, and biodiesel was produced with a yield of 99.20%. Further quality parameter testing of the biodiesel obtained density, kinematic viscosity, acid number, iodine number, cetane number, total glycerol content, and methyl ester content of biodiesel were 861.12 kg/m^3, 5.38 mm^2/s, 2.88 mg KOH/g, 63.45 g I_2/100 g, 62.51, 0.29%, and 95.37%, respectively.

1. Introduction

Economic activities across various sectors have increased public mobility, leading to greater transportation demand and energy consumption, particularly from conventional fossil fuels. The use of petroleum-based fossil fuels in the transportation sector reportedly produces 29% of total carbon dioxide (CO_2) emissions [1]. As a major component of "greenhouse gases", CO_2 emissions are directly responsible for climate change and global temperature increases [2]. Therefore, transitioning to renewable energy sources to support economic activities has become increasingly important. Biodiesel is one such alternative, offering several potential benefits when used as a transportation fuel, including reduced environmental and public health impacts, improved engine lubrication, an increased cetane number, and enhanced transportation system resilience [3].

Biodiesel, or fatty acid alkyl esters, is produced from various sources of fatty acids as raw materials, such as vegetable oils and animal fats, through esterification and/or transesterification reactions with the help of catalysts [4]. Gebremariam and Marchetti [4] further stated that the characteristics of the biodiesel produced depend on the characteristics of the raw materials and reaction conditions, such as the mole ratio of alcohol to oil, the type and amount of catalyst, the reaction temperature, and the reaction time.

In terms of raw materials, raw material procurement has the greatest impact on biodiesel production costs, accounting for approximately 42–69% of total

production costs [5]. Therefore, using non-edible oils as a source of fatty acids has the potential to reduce the total cost of biodiesel production. One type of non-edible oil is palm acid oil (PAO). PAO is a component found in POME (palm oil mill effluent), the liquid waste from the palm oil refining process. Processing one ton of fresh oil palm fruit bunches produces approximately 60% POME, consisting of approximately 4–5% total solids, including PAO [6, 7]. TradeAsia reports that PAO is composed of 50–80% free fatty acids (FFA), 10–40% triglycerides, and 1–3% water [8].

High FFA content in oil feedstocks can promote saponification during biodiesel production using homogeneous base catalysts, such as KOH and NaOH, thereby reducing catalyst effectiveness and overall production efficiency.[4]. In contrast, acid catalysts are insensitive to the presence of FFA; therefore, these catalysts are especially suitable for oils with low triglyceride content and higher FFA [9]. The use of homogeneous acids, generally sulfuric acid (H_2SO_4) and hydrochloric acid (HCl), is effective in assisting the reaction, these acids are corrosive, more difficult to separate from the reaction product mixture, less environmentally friendly (toxic), and cannot be reused. The disadvantages of homogeneous acid catalysts can be overcome by the use of solid acid catalysts [10]. One potential solid acid catalyst is sulfonated activated carbon from rice husks.

Rice husk is a waste product of the rice milling process. Rice husk contains an average of 33.43% cellulose, 20.99% hemicellulose, 18.25% lignin, and 17.45% silica [11]. The cellulose, hemicellulose, and lignin in rice husk undergo carbonization at 460–475°C, producing rice husk charcoal with a carbon content of approximately 48.89% [12]. The carbon in rice husk charcoal, after being purified of silica (activated), is then modified by sulfonation and can be used as a solid acid catalyst [13]. In addition, the method of charcoal activation from biomass and sulfonation techniques have been reported to influence the physical and chemical characteristics of the resulting sulfonated activated carbon [14].

Compared with other biomass sources such as coconut shells, fruit peels, and wood, rice husks, with their very high silica content, impart various structural and chemical advantages to the resulting activated carbon after silica is removed via leaching [15]. Rice husk char purified of silica through leaching yields carbon characterized by abundant mesoporous and macroporous structures, thereby enhancing molecular accessibility, as well as a significantly increased specific surface area [16], higher total pore volume [17], and an abundance of surface oxygen functional groups [18] to make the sulfonation process more intensive and effective.

Biodiesel synthesis from PAO using a solid acid catalyst in the form of sulfonated activated carbon has not been widely reported. Widayat *et al.* [19] produced biodiesel from PAO using Fe/zeolite as the catalyst. PAO in the form of POME has been used as a raw material in biodiesel production using a sulfuric acid catalyst [20] and a sulfonated carbon-silica catalyst from rice husks [21].

Therefore, this study synthesized, characterized, and tested the catalytic activity of sulfonated activated carbon from rice husk for the synthesis of biodiesel from PAO. In this study, the sulfonation technique for activated carbon from rice husk was carried out using conventional heating. The aim of this study was to determine the optimum conditions for biodiesel synthesis from PAO using sulfonated activated carbon from rice husk as a catalyst.

2. Experimental

The research was conducted in five stages: (1) characterization of PAO; (2) preparation and characterization of activated carbon derived from rice husk; (3) sulfonation and characterization of the rice husk-derived activated carbon; (4) synthesis and characterization of biodiesel under various reaction conditions; and (5) comparison of biodiesel quality with established standards. Each stage involved specific equipment, analytical instruments, materials, and procedures.

2.1. Equipment and Materials

The main equipment used to prepare sulfonated activated carbon from rice husk included a muffle furnace (Nabertherm, Germany; maximum temperature of 3000°C), a 250 mL neck flask reactor equipped with a condenser, a heating mantle with a magnetic stirrer (Thermo Scientific, USA; maximum temperature of 350°C), a Büchner funnel, a mortar, a sieve and sieving machine, and a separatory funnel. Analytical instruments used for sample characterization included a pycnometer, an Ostwald viscometer, titration apparatus, an X-ray fluorescence (XRF) spectrometer (Rigaku Supermini200, Japan), a Brunauer–Emmett–Teller (BET) surface area analyzer (Quantachrome Quadrasorb EVO, USA), and a Fourier-transform infrared (FTIR) spectrometer (PerkinElmer UATR Spectrum Two, USA).

Rice husks obtained from a rice mill in Sumedang, West Java, Indonesia, served as the carbon precursor. PAO, the feedstock for biodiesel production, was obtained from the palm oil processing plant of PT Agriclinal, Bengkulu, Indonesia. Hydrochloric acid (HCl, 3.0 M; Merck), sodium carbonate (Na_2CO_3, analytical grade; Merck), and potassium carbonate (K_2CO_3, analytical grade; Merck) were used in the activation of the carbon. Methanol (CH_3OH, analytical grade; Merck) served as the alcohol in the esterification reaction. Other analytical-grade chemicals from Merck were used for titrimetric analyses.

2.2. Experiment

2.2.1. Preparation of Activated Carbon from Rice Husk

After being washed with tap water, the rice husks were drained, dried, ground, and sieved to obtain rice husks with a 250-mesh size. The rice husk powder was then pyrolyzed for 2 hours at 550°C in a muffle furnace at a heating rate of 10°C/minute under nitrogen gas. The

pyrolysis of rice husks produced rice husk char, with carbon and silica as the main components.

The procedure for preparing activated carbon from rice husks was carried out as described by Yeletsky *et al.* [22]. The carbon in the rice husk char was then separated from silica and other impurities via activation to obtain activated carbon. In this study, the activation of rice husk char was performed using the alkali fusion method. Rice husk charcoal and a mixture of alkali carbonate salts (Na_2CO_3 and K_2CO_3 with a molar ratio of 1:1) were heated at a temperature of 900°C with a heating rate of 10°C/minute in a muffle furnace for 3 hours in an inert medium (nitrogen gas). In the activation stage, a mixture of carbonate salts was used at up to 4:1 (w/w) relative to the silica in the rice husk charcoal. The selection of an equimolar ratio (1:1) for the Na_2CO_3 and K_2CO_3 mixture was based on specific technical considerations.

Briefly, this equimolar ratio corresponds to the eutectic point, where the melting temperature of the salt mixture is lower (710°C) than that of the pure salts (851°C for Na_2CO_3 and 891°C for K_2CO_3) [23]. Consequently, as the mixture transitions to a liquid phase, ion mobility [24], synergistic ionic effects [25], and chemical reactivity [26] increase at lower temperatures. Meanwhile, the activation temperature and duration were selected as 900°C and 3 hours, respectively, because these parameters, particularly the temperature, represent the reported optimum conditions for activation. Under these optimum conditions, a balance is achieved among the specific surface area, porosity, and surface chemical properties (including the density of oxygen-containing functional groups) of the resulting activated carbon [24].

Activated carbon from activated rice husk charcoal (AC_{RH}) was cooled to room temperature, washed with deionized water until neutral pH, then washed with 3 M HCl solution and again with deionized water until neutral pH. The activated carbon was dried at 120°C for 12 hours in an oven, then cooled to room temperature and stored for sulfonation in the next stage of catalyst preparation.

2.2.2. Preparation and Characterization of Sulfonated Activated Carbon from Rice Husk

Sulfonation of rice husk-derived activated carbon to produce a solid acid catalyst was performed according to the procedure reported by Zeng *et al.* [25]. The activated carbon was mixed with a 98% H_2SO_4 solution at a 1:10 (w/v) ratio in a reactor flask equipped with a reflux condenser. The mixture was heated with a heating mantle with a magnetic stirrer in an inert nitrogen gas medium at 150°C for 8 hours at a stirring speed of 400 rpm. After sulfonation, the resulting solid was purified by filtration, washing, and drying.

The synthesized sulfonated activated carbon, hereafter denoted as AC_{RH}-SO_3H, was characterized in terms of its functional groups using FTIR spectroscopy, acid site density using acid–base titration [26], and specific surface area and pore size distribution using the BET method.

2.2.3. Biodiesel Synthesis from PAO: Catalytic Performance and Product Characterization

The final step was to evaluate the catalyst performance of AC_{RH}-SO_3H for biodiesel synthesis from PAO. Before characterization, PAO was heated at 110°C for 30 minutes to melt the oil and remove its moisture. PAO was then characterized to determine its density (at 40°C), acid value, saponification value, water content, total glycerol content, and solid impurity content. The molar mass of PAO for the purpose of preparing the mole ratio between PAO and methanol was calculated using Equation (1) [27].

$$Molar\ mass\ of\ PAO = \frac{56.1 \times 1000 \times 3}{(SN - AN)} \quad (1)$$

Where, the molar mass of PAO is in g/mol, and *SN* and *AN* are respectively the saponification number and acid number in mg KOH/g.

PAO was added and mixed with methanol in the reactor flask at various mole ratios of PAO to methanol of (1:16), (1:24), and (1:32). The AC_{RH}-SO_3H catalyst was added to the reactor at various concentrations of 2, 3, and 5% (w/w) relative to PAO. The reaction was carried out at 65°C for 2 hours at a stirring speed of 600 rpm [28]. After purification of the reaction product, the catalytic performance of AC_{RH}-SO_3H was evaluated using reaction conversion parameters and biodiesel yield. The reaction conversion, as an indicator of the amount of FFA converted into biodiesel, was calculated by Equation (2), while the biodiesel yield was calculated based on Equation (3). In addition, the catalytic performance of AC_{RH}-SO_3H as a heterogeneous acid catalyst in the PAO esterification reaction was compared with that of the homogeneous acid catalyst H_2SO_4.

$$Conversion\ of\ FFA = \frac{AN\ PAO - AN\ biodiesel}{AN\ PAO} \times 100\% \quad (2)$$

$$Yield\ of\ biodiesel = \frac{weight\ of\ biodiesel}{weight\ of\ PAO} \times 100\% \quad (3)$$

Biodiesel produced under the optimum reaction conditions (PAO-to-methanol molar ratio and catalyst loading) was further characterized to assess its quality. The quality parameters of biodiesel were tested using procedures according to SNI 7182:2024, including density and kinematic viscosity at 40°C, acid number, iodine number, free glycerol content, and methyl ester content. The cetane number was calculated using the approach reported by Azam *et al.* [29] and Equation (4).

$$Cetane\ number = 46.3 + \frac{5458}{SN} - 0.225\ IN \quad (4)$$

Where, *SN* is the saponification number, and *IN* is the iodine number in units of mg KOH/g and g I_2/100 g, respectively.

3. Results and Discussion

The research results and their discussion are presented sequentially, starting with the characteristics of PAO, the characteristics of activated carbon from rice husk, the characteristics of AC_{RH}-SO_3H, the performance of biodiesel synthesis from PAO using the AC_{RH}-SO_3H catalyst, and ending with the specifications of biodiesel quality.

3.1. Characteristics of PAO

Before biodiesel synthesis, PAO was characterized to determine its initial properties. The results of the analyses are presented in Table 1. The PAO used as the feedstock in this study had an acid value of 19.30 mg KOH/g (Table 1). Assuming that the FFAs were predominantly oleic acid (molar mass of 282.47 g/mol), the FFA content was calculated to be 9.72%. Because the FFA content exceeded 2%, an acid catalyst was recommended for biodiesel production [9].

The PAO characteristic data in Table 1 also show a soap value of 189.33 mg KOH/g. This soap value, combined with the acid value, was used to calculate the molar mass of triglycerides or neutral oils in the PAO. PAO with a soap number of 189.33 mg KOH/g and an acid number of 19.30 mg KOH/g, based on Equation (1), the molar mass of triglycerides from PAO is 989.82 g/mol. According to the data in Table 1, the impurity components in PAO, namely water, total glycerol, and solids, are relatively small in content. Therefore, in this study, it is assumed that they do not interfere with the performance of biodiesel synthesis.

As a comparison of characteristics, Bahadi *et al.* [30] reported that crude palm oil (CPO) with high FFA content had a density, acid value, saponification value, and water content of 878 kg/m^3, 21.3 mg KOH/g, 203.1 mg KOH/g, and 0.6%, respectively. Therefore, the molar mass of triglycerides of the CPO was 952.74 g/mol. In addition, the FFA content was reported at 9.4%. CPO with high FFA content can be said to be a type of palm-based oil similar to PAO. Therefore, PAO in this study has quite similar characteristics to the CPO from the research results of Bahadi *et al.* [30].

3.2. Characteristics of AC_{RH}

Rice husk was carbonized to produce rice husk charcoal as the precursor for activated carbon. The carbonization process yielded approximately 37.80% rice husk charcoal. Analysis of the ash content showed that the charcoal contained an average of 54.44% ash, indicating a carbon content of 45.56%. In addition to silica (SiO_2), the ash contained other metal oxide impurities. These impurities needed to be removed to obtain activated carbon with a higher carbon content. In this study, metal oxide impurities other than silica were removed by leaching with an HCl solution, followed by silica removal through alkali fusion.

Table 1. PAO characteristics

Parameters	Unit	Value
Density at 40°C	kg/m^3	897.93
Acid number	mg KOH/g	19.30
Saponification number	mg KOH/g	189.33
Moisture content	%	4.27
Total glycerol content	%	0.35
Solid impurity content	%	0.11

Table 2. Composition of rice husk charcoal before and after leaching with HCl solution

Oxide compound	Content (%)*	
	Before leaching	After leaching
SiO_2	98.451	99.748
K_2O	0.771	0.028
CaO	0.520	0.171
FeO	0.097	0.043
BeO	0.007	0.002
MnO	0.004	0.004
SrO	0.002	0.002
Rb_2O	0.001	0.001
ZnO	0.001	0.001

*The composition of oxide compounds is based on the ash weight of rice husk charcoal

During HCl leaching, metal oxides other than silica reacted with the acid to form soluble chloride salts, thereby facilitating their removal from the carbon. For example, K_2O and CaO impurities were removed through the reactions presented in Equations (5) and (6), respectively. The composition of rice husk charcoal before and after leaching was determined using XRF analysis. The results are presented in Table 2.

$$K_2O_{(s)} + 2HCl_{(aq)} \rightarrow 2KCl_{(aq)} + H_2O_{(l)} \quad (5)$$

$$CaO_{(s)} + 2HCl_{(aq)} \rightarrow CaCl_{2(aq)} + H_2O_{(l)} \quad (6)$$

The collection of all oxide compounds measured by XRF in Table 2 represents the ash from rice husk charcoal. Carbon, a light element with a low fluorescence photon energy of approximately 0.28 keV, is not detected [31]. The research data in Table 2 show that leaching of rice husk charcoal has successfully separated impurities from carbon, excluding SiO_2. The K_2O content in rice husk charcoal was successfully reduced from 0.771% to 0.028%, corresponding to a K_2O separation rate of around 96.37%. Meanwhile, the degree of separation of CaO from rice husk charcoal was approximately 67.12%. During the HCl leaching stage on rice husk charcoal, the reduction of impurities other than SiO_2 resulted in rice husk charcoal with an ash portion containing 99.748% SiO_2.

From the results of the previous stage of rice husk charcoal preparation, rice husk charcoal with an ash content of 54.44% was obtained. Because the results of the XRF analysis showed that the silica content in the ash was 99.748%, the silica content in the rice husk charcoal was 54.30% (the result of multiplying the ash fraction in the rice husk charcoal by the silica content in the ash). The estimated silica content was then used to calculate the amount of carbonate salt required for subsequent activation via alkali fusion.

The next stage in preparing AC_{RH} involved alkali fusion of the rice husk charcoal. This process aimed to convert SiO_2 into soluble alkali silicates by reacting it with a mixture of alkali carbonate salts, particularly K_2CO_3 and Na_2CO_3, under solid-state reaction conditions, as represented by Equation (7), where M denotes K or Na [22].

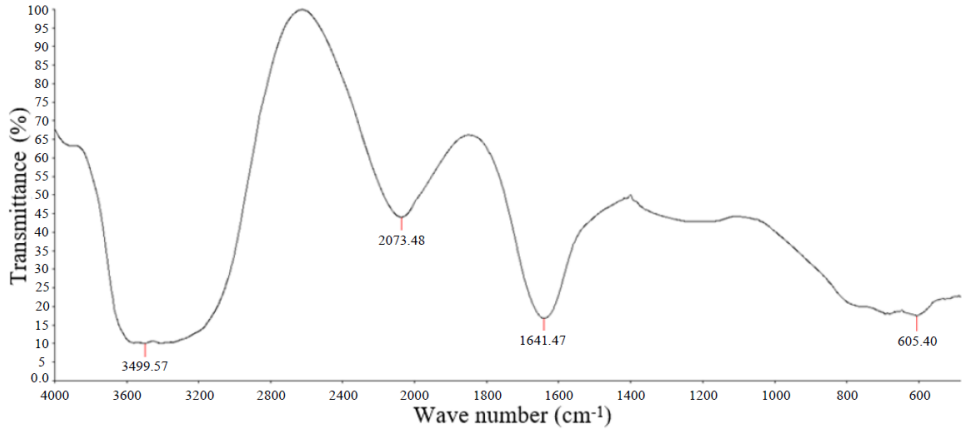


Figure 1. FTIR spectrum of AC_{RH}

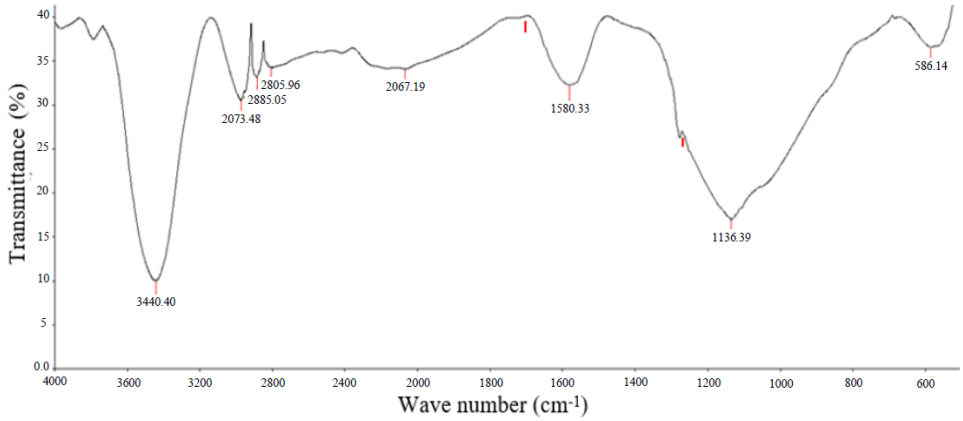


Figure 2. FTIR spectrum of AC_{RH}-SO_3H

$$M_2CO_{3(s)} + SiO_{2(s)} \rightarrow M_2SiO_{3(l)} + CO_{2(g)} \quad (7)$$

During the alkali fusion of rice husk charcoal, silica was converted into potassium and sodium silicates, facilitating its removal and exposing the inner and outer carbon surfaces, thereby increasing the accessible surface area [32]. The effectiveness of alkali fusion activation was evaluated by characterizing the functional groups of the resulting AC_{RH} using FTIR spectroscopy. The FTIR spectrum of AC_{RH} is presented in Figure 1.

The FTIR spectrum of A_{CRH} in Figure 1 shows no longer sharp absorption bands at wavenumbers 1092, 793, and 547 cm^{-1}. The absorption bands at wavenumbers 1092, 793, and 547 cm^{-1} respectively indicate functional groups of asymmetric stretching vibrations of siloxane Si–O–Si, tetrahedral or orthosilicate vibrations of SiO_4, and bending vibrations of siloxane Si–O–Si [33, 34]. Therefore, the activation stage using alkali fusion can be considered successful for separating silica impurities from rice husk charcoal and producing AC_{RH}. However, an FTIR absorption band is still found at wavenumber 3499.57cm^{-1}, which indicates the presence of Si–OH hydrogen bonds [33]. This indicates that residual silica remains in AC_{RH}.

3.3. Characteristics of AC_{RH}-SO_3H

Sulfonation of AC_{RH} was performed to introduce sulfonic acid groups (–SO_3H) onto its surface, thereby increasing its acidity. Sulfonic acid groups are strong Brønsted–Lowry acid sites that act as proton donors [35]. Sulfuric acid is commonly used as a sulfonating agent to introduce these groups. The acid site density of AC_{RH} before and after sulfonation (AC_{RH}-SO_3H) was compared based on acid site density, as presented in Table 3. Sulfonation increased the acid site density from 0.52 to 6.87 mmol SO_3H/g. This substantial increase in acid site density is expected to enhance the catalytic activity of AC_{RH}-SO_3H in biodiesel synthesis from PAO.

In addition to the increase in acid site density, the success of the sulfonation stage was confirmed by FTIR characterization. The FTIR absorption bands of AC_{RH}-SO_3H are shown in Figure 2. The absorption band at wave number 1136 cm^{-1} indicates the presence of functional groups with sulfur content on the surface of activated carbon, namely in the form of symmetric and asymmetric stretching of –SO_2. While the absorption band at wave number 3440 cm^{-1} shows the stretching vibration of the (–OH) group, which may be in the form of (–S=O)$_2$(OH) or –COOH groups [25]. The presence of oxygenate functional groups, such as –COOH and –OH, is possible to form through the oxidation of carbon supports by strong oxidizing sulfonation agents such as concentrated H_2SO_4, oleum, and SO_3 gas [32].

Table 3. Acid site density of AC_{RH} and AC_{RH}-SO_3H

Sample	Acid site density (mmol SO_3H/g)
AC_{RH}	0.52
AC_{RH}-SO_3H	6.87

Table 4. Surface characterization results of AC_{RH}-SO_3H

Surface area (m^2/g)	Average pore volume (cm^3/g)	Average pore radii (Å)	Reference
1430	3.299	9.23	This study
1233	0.744	-	[25]

Further characterization of AC_{RH}-SO_3H was carried out by measuring the specific surface area and pore size distribution using the BET adsorption model. The results of this characterization and their comparison with those of other researchers are shown in Table 4. AC_{RH}-SO_3H from this study has a larger surface area and pore volume than those reported in the comparative study (Table 4). These results indicate that the activation stage of AC_{RH} in this study was more successful than that of Zeng *et al.* [25]. Surface area, pore volume, and pore radius play important roles in determining the performance of a catalyst material. Large surface area and pore volume, as well as pore radius that matches the size of the reactant and product molecules, are generally proportional to the increase in the performance of a catalyst in accelerating the reaction rate [36].

The synthesis of biodiesel from PAO involves reactants including triglycerides, FFAs with various fatty acids, and methanol. While the reaction products consist of biodiesel (methyl esters of fatty acids), water, and glycerol. Methanol has a molecular radius of 1.8 Å (Angstrom, 1 Å = 10−10 m) [37]. FFAs in palm oil, such as palmitic, myristic, stearic, oleic, and linoleic acids, have molecular radii between 1.86–4.50 Å, and triglycerides in palm oil are around 29.0 Å [38]. The molecular radii of methanol and FFAs are smaller than the average pore radius of AC_{RH}-SO_3H (9.23 Å), suggesting that these molecules can access the catalyst's internal active sites. Consequently, the esterification of FFAs with methanol may occur within the catalyst pores, potentially enhancing biodiesel formation. In contrast, the larger triglyceride molecules are unlikely to enter most of the pores, suggesting that their transesterification with methanol occurs predominantly on the external catalyst surface.

3.4. Catalytic Performance of AC_{RH}-SO_3H in PAO-Derived Biodiesel

3.4.1. Comparison of AC_{RH}-SO_3H and H_2SO_4 in Reducing the Acid Number of PAO

Reducing the acid number in biodiesel production is generally achieved, especially on a commercial scale, using homogeneous acid catalysts such as concentrated H_2SO_4. Therefore, in this study, AC_{RH}-SO_3H was compared with concentrated H_2SO_4 in reducing the acid number of PAO. The test was carried out at a mole ratio between PAO and methanol of (1:32), a catalyst loading of 2% w/w (for AC_{RH}-SO_3H) and 1% v/v (for concentrated H_2SO_4) relative to PAO, a reaction temperature of 65°C, and a reaction time of 2 hours. The initial acid number of PAO was 19.30 mg KOH/g (Table 1). The results of the performance test are shown in Figure 3.

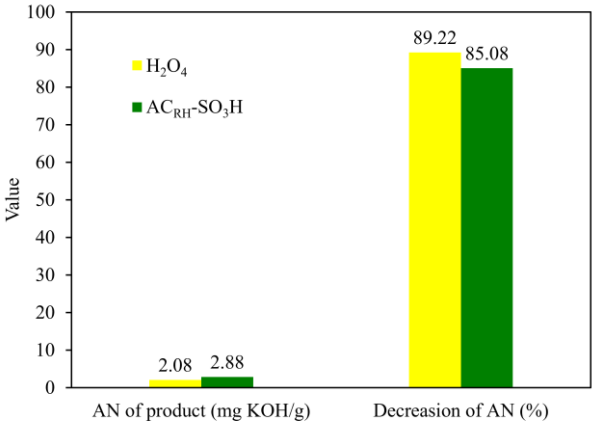


Figure 3. Comparison of the performance of H_2SO_4 and AC_{RH}-SO_3H as catalysts to reduce acid number

The results of the catalyst performance test, as shown in Figure 3, show that AC_{RH}-SO_3H has a performance that is quite close to that of concentrated H_2SO_4 in reducing the acid number of PAO. With the ability of the AC_{RH}-SO_3H catalyst to reduce the acid number of PAO by 85.08%, while concentrated H2SO4 is 89.22%, the difference in performance of AC_{RH}-SO_3H in reducing the acid number of PAO is only about 4.65% lower than that of concentrated H_2SO_4. Therefore, as a solid-acid heterogeneous catalyst, AC_{RH}-SO_3H is a promising catalyst based on several considerations.

3.4.2. Effect of the PAO-to-Methanol Molar Ratio on FFA Conversion

The molar ratio of PAO to methanol is an important factor influencing biodiesel synthesis. An insufficient methanol ratio may limit the reaction rate and conversion, whereas an excessive ratio may increase production costs and reduce process efficiency. To evaluate the catalytic performance of AC_{RH}-SO_3H at different PAO-to-methanol molar ratios, the reactions were conducted using a catalyst loading of 2 wt% at 65°C for 2 hours. The FFA conversion was calculated using Equation (2). The initial acid number of PAO was 19.30 mg KOH/g. The acid number value of the reaction products and the corresponding FFA conversion percentages at each molar ratio are presented in Table 5 and Figure 4.

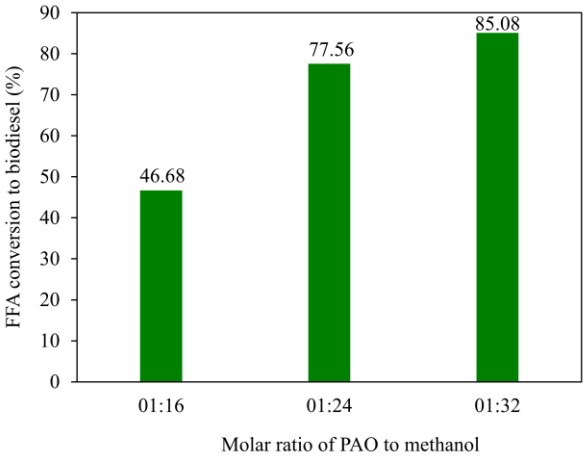


Figure 4. Effect of PAO/methanol molar ratio on AC_{RH}-SO_3H catalyst performance

Table 5. Acid number of PAO and reaction product, and degree of FFA conversion at the PAO/methanol molar ratio test

PAO to methanol molar ratio	Acid number (mg KOH/g)		FFA conversion (%)
	PAO	Reaction product	
1:16	19.30	10.29	46.68
1:24		4.33	77.56
1:32		2.88	85.08

The research data in Table 5 and Figure 4 show that increasing methanol use improves the performance of the AC_{RH}-SO_3H catalyst in converting FFA to biodiesel. From a chemical kinetics perspective, this occurs because using a larger amount of reactant, in this case is methanol, increases the probability of effective collisions between reactants, thereby accelerating the reaction rate at which FFAs in PAO are converted into biodiesel. Thermodynamically, an excess of methanol shifts the reaction equilibrium toward fatty acid methyl ester formation, in accordance with Le Chatelier's principle. This shift favors product formation but does not prevent the reverse reaction. Because AC_{RH}-SO_3H is a heterogeneous catalyst, its surface properties and the accessibility of its active sites may also influence FFA conversion. However, the observed relationship between the PAO-to-methanol molar ratio and FFA conversion alone is insufficient to establish whether the catalyst provides adequate surface area for reactant adsorption.

3.4.3. Effect of Catalyst Loading on FFA Conversion

Catalyst loading is another important factor influencing catalytic reaction performance. In this study, the effect of catalyst loading on FFA conversion was evaluated at three levels: 2, 3, and 5 wt% relative to the mass of PAO. The results presented in Table 6 and Figure 5 indicate that catalyst loading did not have a consistent effect on FFA conversion over the AC_{RH}-SO_3H catalyst. Increasing the catalyst loading from 2 to 3 wt% decreased FFA conversion from 85.08% to 82.69%. However, increasing the loading to 5 wt% raised FFA conversion to 83.58%, although this value remained lower than that obtained with 2 wt% catalyst. In principle, increasing catalyst loading provides more active sites for the reaction, potentially enhancing the conversion of reactants to products. However, this improvement may not be proportional to the amount of catalyst added.

Table 6. Acid number of PAO and reaction product, and degree of FFA conversion at the catalyst loading test

Catalyst loading (%)	Acid number (mg KOH/g)		FFA conversion (%)
	PAO	Reaction product	
2	19.30	2.88	85.08
3		3.34	82.69
5		3.17	83.58

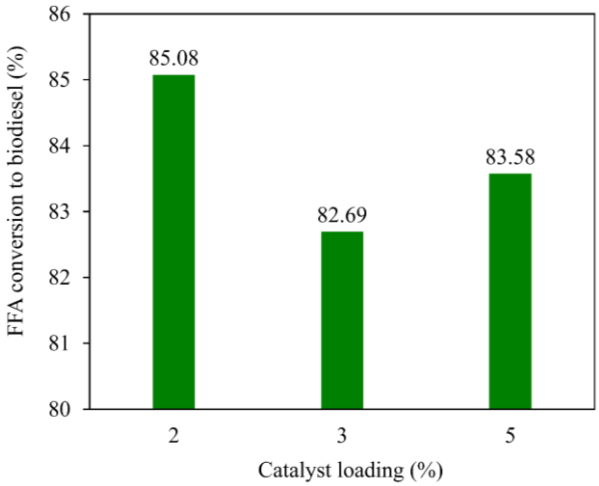


Figure 5. The effect of catalyst loading on the performance of the AC_{RH}-SO_3H catalyst

The anomalous results produced in this study are suspected to be due to a combination of deficiencies in catalyst characteristics and in the fluid dynamics of the reactant-catalyst mixture. In this study, the Biodiesel synthesis from PAO was conducted in a stirred-tank reactor at a fixed stirring speed. Increasing the catalyst content requires a higher dispersion energy in the reactant-catalyst mixture to maintain catalytic reaction performance. In addition, more detailed characteristics of the catalyst, such as the degree of particle-size homogeneity, the distribution of active sites for the reaction, and the degree of agglomeration, also affect its catalytic performance.

Increasing the usage of solid heterogeneous catalysts beyond the optimum limit in liquid-solid reaction systems has been reported to strengthen attractive forces between catalyst particles, thereby causing local catalyst agglomeration [39]. This local agglomeration subsequently triggers a significant reduction in the catalyst's specific surface area and the blocking of active sites, while also limiting the diffusive mass transfer of reactant and product molecules during the reaction [40]. Therefore, the inconsistency between the AC_{RH}-SO_3H catalyst content and the degree of FFA conversion to biodiesel is suspected to be due to fluctuations in the effectiveness of interactions between reactant molecules and catalyst particles.

Based on the study of the influence of the PAO-to-methanol molar ratio and catalyst loading that has been described, it can be concluded that the optimal catalytic performance of AC_{RH}-SO_3H in the synthesis of biodiesel from PAO is achieved when the reaction is carried out at a PAO-to-methanol molar ratio of 1:32 and a catalyst loading of 2%. Under these reaction conditions, biodiesel is produced with a yield, calculated based on Equation (2), of 99.20% and a conversion degree of FFA to biodiesel of 85.08%.

3.5. Quality Assessment of PAO-Derived Biodiesel

The biodiesel produced under optimum synthesis conditions was then characterized for quality and compared with the biodiesel quality standards stipulated in the Decree of the Director General of New, Renewable

Energy and Energy Conversion (EBTKE) of the Ministry of Energy and Mineral Resources of the Republic of Indonesia Number 195.K/EK.05/DJE/2022 concerning standard specifications for biodiesel (B100). In this study, the quality parameters compared were density, kinematic viscosity, acid value, iodine value, cetane number, total glycerol content, and methyl ester content. The results of the biodiesel quality analysis and its comparison with the biodiesel quality standards according to the Decree of the Director General of EBTKE in 2022 are shown in Table 7.

A comparison of the quality specifications between the biodiesel from this study and the biodiesel standards, as shown in Table 7, shows that the biodiesel from this study meets the standards for density, viscosity, iodine value, and cetane number. However, the quality parameters of acid value, total glycerol content, and methyl ester content do not meet the standards according to the Decree of the Director General of EBTKE in 2022. The acid value and free glycerol content of the biodiesel, two types of impurities, are still above the minimum permissible limits.

The acid number of biodiesel reflects the presence of residual FFAs and other acidic compounds. A value exceeding the maximum limit specified by the quality standard may indicate incomplete conversion of FFAs during esterification. Under the optimum conditions identified in this study (a PAO-to-methanol molar ratio of 1:32 and a catalyst loading of 2 wt%) the acid number of the resulting biodiesel may require further reduction to meet the standard. Other reaction parameters, including reaction time, temperature, and stirring speed, could therefore be investigated to determine their effects on FFA conversion and biodiesel quality and to establish suitable operating conditions.

Table 7. Biodiesel quality from PAO with AC_{RH}-SO_3H catalyst and comparison with standard

Quality parameters	Value of biodiesel	
	This study	EBTKE
Density at 40°C (kg/m³)	861.12	850-890
Viscosity at 40°C (mm²/s)	5.38	2.3-6.0
Acid number (mg KOH/g)	2.88	Max. 0.4
Saponification number (mg KOH/g)	179.05*	-
Iodine number (g I_2/100 g)	63.45	Max. 115
Cetane number	62.51	Min. 51
Total glycerol content (%)	0.29	Max. 0.24
Methyl ester content (%)	95.37	Min. 96.5

* used for the calculation of the cetane number based on Equation (4).

Another type of impurity is glycerol, which is present in biodiesel and is typically a byproduct of the transesterification reaction. Transesterification converts triglycerides in oil into glycerol by reacting them with a simple alcohol, typically methanol or ethanol. The glycerol formed and mixed with biodiesel is typically separated in two stages: sedimentation and water washing. In this study, PAO, as the source of triglycerides and FFA, initially contained 0.35% total glycerol. After undergoing the synthesis stage under the optimum conditions studied and purification, biodiesel was produced with a total glycerol content of 0.29%.

The presence of glycerol in PAO, combined with the glycerol formed from the transesterification reaction, results in a heavier glycerol separation burden. The use of acidified activated carbon in biodiesel synthesis has the potential to facilitate the esterification and transesterification reactions [32]. The glycerol purification stage thought to be responsible for the total glycerol content in biodiesel exceeding the minimum quality standard is the glycerol washing stage. Therefore, the glycerol washing stage needs to be optimized through various efforts, including the biodiesel-to-wash water ratio, washing temperature, number of washing stages, and the washing method or equipment.

4. Conclusion

Sulfonated activated carbon from rice husks has been successfully synthesized and characterized. The presence of sulfonic acid groups in the activated carbon was confirmed by FTIR spectroscopy and by an increase in acid site density. The resulting sulfonated activated carbon exhibited adequate characteristics as a catalyst for biodiesel synthesis from PAO, as indicated by acid site density parameters and surface characteristics determined by the BET adsorption method. Testing the catalytic performance of sulfonated activated carbon from rice husks in biodiesel synthesis from PAO showed that catalyst performance was influenced by the PAO-to-methanol molar ratio and catalyst loading. Optimal catalytic performance was achieved when the biodiesel synthesis reaction was carried out at a PAO-to-methanol molar ratio of 1:32 and a catalyst loading of 2%, with specific reaction temperature, reaction time, and stirring speed. From an operational standpoint, the issue of high acid values, or elevated free fatty acid (FFA) content, in biodiesel can be addressed by repeating the reaction until the standard acid value specification is met. Meanwhile, reducing the glycerol content in biodiesel can be achieved by intensifying the purification of glycerol during the biodiesel washing and glycerol decantation stages.

Acknowledgment

We would like to express our gratitude to Ibnu Alif Nugraha for his contribution to data collection. We also extend our gratitude to the Head of the Physical Chemistry Laboratory, Department of Chemistry, Faculty of Mathematics and Natural Sciences, Universitas Padjadjaran, for facilitating access to laboratory facilities, which enabled this research to be completed.

References

[1] Shemelis Nigatu Gebremariam, Biodiesel as a transport fuel, advantages and disadvantages: review, *Biofuels, Bioproducts and Biorefining*, 17, 5, (2023), 1445-1456 https://doi.org/10.1002/bbb.2503

[2] Tonmoy Choudhury, Umar Nawaz Kayani, Azeem Gul, Syed Arslan Haider, Sareer Ahmad, Carbon emissions, environmental distortions, and impact on growth, *Energy Economics*, 126, (2023), 107040 https://doi.org/10.1016/j.eneco.2023.107040

[3] U. S. Department of Energy, Biodiesel Benefits and Considerations, https://afdc.energy.gov/fuels/biodiesel-benefits

[4] Shemelis Nigatu Gebremariam, Jorge Mario Marchetti, Biodiesel production technologies: review, *AIMS Energy*, 5, 3, (2017), 425-457 https://doi.org/10.3934/energy.2017.3.425

[5] Tenny Kristiana, Adrian O'Connell, Chelsea Baldino, *Produksi biodiesel berkualitas tinggi dari minyak jelantah di Indonesia*, International Council on Clean Transportation, 2023

[6] Noor-Afiqah Ahmad Zain, Kar Ling Tan, Prihardi Kahar, Chiaki Ogino, Lipid production from palm acid oil (PAO) as a sole carbon source by Meyerozyma guilliermondii, *Processes*, 13, 2, (2025), 311 https://doi.org/10.3390/pr13020311

[7] Ashfaq Ahmad, Azizul Buang, Aamir Hussain Bhat, Renewable and sustainable bioenergy production from microalgal co-cultivation with palm oil mill effluent (POME): a review, *Renewable and Sustainable Energy Reviews*, 65, (2016), 214-234 https://doi.org/10.1016/j.rser.2016.06.084

[8] TradeAsia, Palm Acid Oil for Oleochemical Industry, (2025),

[9] Basir Maleki, S. Siamak Ashraf, Mohsen Mansouri, Comparison of catalysts types performance in the generation of sustainable biodiesel via transesterification of various oil sources: a review study, *Materials Today Sustainability*, 18, (2022), 100157 https://doi.org/10.1016/j.mtsust.2022.100157

[10] S. T. Keera, Seham M. El sabagh Sabagh, A. R. Taman, Transesterification of vegetable oil to biodiesel fuel using alkaline catalyst, *Fuel*, 90, 1, (2011), 42-47 https://doi.org/10.1016/j.fuel.2010.07.046

[11] Ali Abbas, Santosh Ansumali, Global Potential of Rice Husk as a Renewable Feedstock for Ethanol Biofuel Production, *Bioenergy Research*, 3, 4, (2010), 328-334 https://doi.org/10.1007/s12155-010-9088-0

[12] Karan Homchat, Sanchai Ramphueiphad, The continuous carbonisation of rice husk on the gasifier for high yield charcoal production, *Results in Engineering*, 15, (2022), 100495 https://doi.org/10.1016/j.rineng.2022.100495

[13] Wendy C. Mateo, Hanwu Leix, Elmar Villota, Moriko Qian, Yunfeng Zhao, Erguang Huo, Qingfa Zhang, Xiaona Lin, Chenxi Wang, Zhiyang Huang, Synthesis and characterization of sulfonated activated carbon as a catalyst for bio-jet fuel production from biomass and waste plastics, *Bioresource Technology*, 297, (2020), 122411 https://doi.org/10.1016/j.biortech.2019.122411

[14] Thiago Alves Lopes Silva, Adilson Candido da Silva, Daniel Pasquini, Synthesis and characterization of acid-activated carbon prepared from sugarcane bagasse for furfural production in aqueous media, *Catalysts*, 13, 10, (2023), 1372 https://doi.org/10.3390/catal13101372

[15] R. Verma, A. G. Nguyen, Preparation and synthesis of rice husk-based activated carbon, in: H.S. Min, H.S. Kusuma, Y.C. Sharma (Eds.) *Recent Advances in Activated Carbon*, CRC Press, Boca Raton, 2024, https://doi.org/10.1201/9781003488606-12

[16] Nurlan Idrissov, Madina Bissenova, Manshuk Mambetova, Mukhtar Yeleuov, Kydyr Askaruly, Arman Umirzakov, Gaukhar Yergaziyeva, Olga Tsurtsumia, Aigerim Serik, Chingis Daulbayev, Rice husk–derived activated carbon and SiO_2–based materials for dye removal and CO_2 adsorption, *South African Journal of Chemical Engineering*, 57, (2026), 100870 https://doi.org/10.1016/j.sajce.2026.100870

[17] Jong-Hoon Lee, Young-Jung Heo, Soo-Jin Park, Effect of silica removal and steam activation on extra-porous activated carbons from rice husks for methane storage, *International Journal of Hydrogen Energy*, 43, 49, (2018), 22377-22384 https://doi.org/10.1016/j.ijhydene.2018.10.039

[18] Cristina Deiana, Dolly Granados, Rosa Venturini, Alejandro Amaya, Marta Sergio, Néstor Tancredi, Activated Carbons Obtained from Rice Husk: Influence of Leaching on Textural Parameters, *Industrial & Engineering Chemistry Research*, 47, 14, (2008), 4754-4757 https://doi.org/10.1021/ie071657x

[19] Widayat Widayat, Rani Amelia Sumarno, Yufridha Yuni Ananda, Sulardjaka Sulardjaka, Hadiyanto Hadiyanto, Faustina Alda Nurushofa, Biodiesel production from PAO-bulk using Fe/zeolite catalyst by wet impregnation method, (2024), https://doi.org/10.2139/ssrn.5067284

[20] Suardi Suardi, Moch Purwanto, Aung Ye Kyaw, Wira Setiawan, Muhammad Uswah Pawara, Alfawan, Biodiesel production from POME (palm oil mill effluent) and effects on diesel engine performance, *International Journal of Marine Engineering Innovation and Research*, 7, 4, (2025), 292-299 https://doi.org/10.12962/j25481479.v7i4

[21] Winnie Sinan Balan, Jidon Janaun, Chin Hing Chung, Veroneka Semilin, Zongyuan Zhu, Stephanie K. Haywood, Dalila Touhami, Khim Phin Chong, Abu Zahrim Yaser, Ping Chin Lee, Sharif H. Zein, Esterification of residual palm oil using solid acid catalyst derived from rice husk, *Journal of Hazardous Materials*, 404, (2021), 124092 https://doi.org/10.1016/j.jhazmat.2020.124092

[22] Petr Yeletsky, Vadim Yakovlev, Maxim Mel'gunov, Valentin N. Parmon, Synthesis of mesoporous carbons by leaching out natural silica templates of rice husk, *Microporous and Mesoporous Materials*, 121, 1–3, (2009), 34-40 https://doi.org/10.1016/j.micromeso.2008.12.025

[23] Dong-yang Zhang, Xue Ma, Hong-wei Xie, Xiang Chen, Jia-kang Qu, Qiu-shi Song, Hua-yi Yin, Electrochemical derusting in molten Na2CO3–K2CO3, *International Journal of Minerals, Metallurgy and Materials*, 28, 4, (2021), 637-643 https://doi.org/10.1007/s12613-020-2068-2

[24] Harry Marsh, Francisco Rodrigues-Reinoso, *Activated Carbon*, Elsevier Science, Amsterdam, 2006,

[25] Danlin Zeng, Qi Zhang, Shiyuan Chen, Shenglan Liu, Guanghui Wang, Synthesis porous carbon-based solid acid from rice husk for esterification of fatty acids, *Microporous and Mesoporous Materials*, 219, (2016), 54-58 https://doi.org/10.1016/j.micromeso.2015.07.028

[26] Manhoe Kim, S. O. Salley, Ka Yuen Simon Ng, Transesterification of Glycerides Using a Heterogeneous Resin Catalyst Combined with a Homogeneous Catalyst, *Energy & Fuels*, 22, 6, (2008), 3594-3599 https://doi.org/10.1021/ef800443x

[27] George Anastopoulos, Ypatia Zannikou, Stamoulis Stournas, Stamatis Kalligero, Transesterification of Vegetable Oils with Ethanol and Characterization of the Key Fuel Properties of Ethyl Esters, *Energies*, 2, 2, (2009), 362-376 https://doi.org/10.3390/en20200362

[28] Surbhi Semwal, Ajai K. Arora, Shanti Prakash, Suresh K. Puri, Deepak K. Tuli, Preparation of novel catalyst composition from natural waste for biodiesel production, *Journal of Scientific & Industrial Research*, 70, 12, (2011), 1054-1060

[29] M. Mohibbe Azam, Amtul Waris, N. M. Nahar, Prospects and potential of fatty acid methyl esters of some non-traditional seed oils for use as biodiesel in India, *Biomass and Bioenergy*, 29, 4, (2005), 293-302 https://doi.org/10.1016/j.biombioe.2005.05.001

[30] Murad Awadh Bahadi, Jumat Salimon, Abd-Wali M. Japir, The physicochemical and thermal properties of Malaysian high free fatty acid crude palm oil, *AIP Conference Proceedings*, Selangor, 2016 https://doi.org/10.1063/1.4966740

[31] Ivan Sverchkov, V. A. Matveeva, Mariia Chukaeva, Determination of carbon, oxygen, hydrogen and nitrogen content in coals using WDXRF scattering spectra, *Spectrochimica Acta Part B: Atomic Spectroscopy*, 207, (2023), 106738 https://doi.org/10.1016/j.sab.2023.106738

[32] Lakhya Jyoti Konwar, Päivi Mäki-Arvela, Jyri-Pekka Mikkola, SO3H containing functional carbon materials: synthesis, structure, and acid catalysis, *Chemical Reviews*, 119, 22, (2019), 11576-11630 https://doi.org/10.1021/acs.chemrev.9b00199

[33] Brian C. Smith, Inorganic III: Even more spectra, and the grand finale, *Spectroscopy*, 39, 03, (2024), 11-15 https://doi.org/10.56530/spectroscopy.hp2485x8

[34] S. K. Saddam Hossain, Lakshya Mathur, Preetam Singh, Ramya Majhi, Preparation of forsterite refractory using highly abundant amorphous rice husk silica for thermal insulation, *Journal of Asian Ceramic Societies*, 5, 2, (2017), 82-87 https://doi.org/10.1016/j.jascer.2017.01.001

[35] Ying Chang, Giuseppe F. Brunello, Jeffrey Fuller, Marilyn Hawley, Yu Seung Kim, Melanie Disabb-Miller, Michael A. Hickner, Seung Soon Jang, Chulsung Bae, Aromatic Ionomers with Highly Acidic Sulfonate Groups: Acidity, Hydration, and Proton Conductivity, *Macromolecules*, 44, 21, (2011), 8458-8469 https://doi.org/10.1021/ma201759z

[36] Xiangyu Fu, Zhenpu Lu, Tianyi Zhao, Donglong Fu, Peng Zhang, Sai Chen, Xinbin Ma, Chunlei Pei, Jinlong Gong, The role of internal diffusion for propane dehydrogenation over Pt-based catalysts, *Chemical Engineering Science*, 317, (2025), 122037 https://doi.org/10.1016/j.ces.2025.122037

[37] Qingli Tang, Zhemin Shen, Christopher K. Russell, Maohong Fan, Thermodynamic and kinetic study on carbon dioxide hydrogenation to methanol over a Ga3Ni5(111) surface: effects of step Edge, *The Journal of Physical Chemistry C*, 122, 1, (2018), 315-330 https://doi.org/10.1021/acs.jpcc.7b08232

[38] Nurul Saadiah Lani, Norzita Ngadi, Mohd Rozainee Taib, Parametric study on the transesterification reaction by using CaO/silica catalyst, *Chemical Engineering Transactions*, 56, (2017), 601-606 https://doi.org/10.3303/CET1756101

[39] Bin-Xin Qiao, Pu He, Yu-Chen Li, Xi-kui Wang, Kai Liu, Wen-Quan Tao, Investigation of the effects of the catalyst structure parameter of an agglomerate model on the performance of a PEM water electrolyzer, *Applied Energy*, 414, (2026), 127842 https://doi.org/10.1016/j.apenergy.2026.127842

[40] María de los Milagros Ballari, Rodolfo Brandi, Orlando Alfano, Alberto Cassano, Mass transfer limitations in photocatalytic reactors employing titanium dioxide suspensions: I. Concentration profiles in the bulk, *Chemical Engineering Journal*, 136, 1, (2008), 50-65 https://doi.org/10.1016/j.cej.2007.03.028